

PAPER • OPEN ACCESS

## Numerical study of heat transfer between impinging gas jets and solid surfaces

To cite this article: Viktor Stoyanov *et al* 2019 *IOP Conf. Ser.: Mater. Sci. Eng.* **618** 012064

View the [article online](#) for updates and enhancements.

# Numerical study of heat transfer between impinging gas jets and solid surfaces

Viktor Stoyanov<sup>1</sup>, Valyo Nikolov<sup>2</sup> and Manuel Mirabal Garcia<sup>3</sup>

<sup>1,2</sup> Technical University of Sofia, Plovdiv Branch,  
Department of Transport and Aviation Equipment and Technologies,  
25 Tsanko Dyustabanov str., 4000 Plovdiv, Bulgaria

<sup>3</sup> The Autonomous University of San Luis Potosí, Institute of Physics,  
64 Alvaro Obregon, Centro, 78300 San Luis, San Luis Potosí, Mexico

E-mail: viktor.stoyanov@gmx.de <sup>1</sup>, vnikolov@tu-plovdiv.bg <sup>2</sup>, mirabal@ifisica.uaslp.mx <sup>3</sup>

**Abstract.** When two spaces of different gas pressure are connected through a nozzle forming and spreading a gas jet with certain energetic characteristics is observed in the region of the lower pressure. If a solid body is located in the region of the jet spreading, then this case is defined as an impinging gas jet. The aim of this work is to consider a specific case of this heat transfer method using 3D virtual simulation models known as Computational Fluid Dynamics - CFD. The simulations were performed in the commercial solver Star-CCM+ version 6.04.014 using two turbulence models: Shear Stress Transport - SST and  $v^2f$  Low-Reynolds Number (Re)  $k-\epsilon$  model. The obtained results are represented by a dimensionless Nusselt number (Nu) and its local validation determines the accuracy of the solver when using a digital twin describing a real measurement set-up with known empirical measurements in digital format.

## 1. Theoretical prerequisites

The first laboratory tests were performed in the 1950s by K Peri [5]. His studies describe the relationship between the temperature and velocity of an impinging jet and the experimental measurements which determine the temperature value on the surface of a dense solid body around which a jet stream flows. Further background analyses and studies were conducted later by H Martin [4], S Beltaos [10] and L W Florschuetz et al. [3], and their documentation refers to the 70s and 80s of the last century. H Martin [4] also performed fundamental research and further developed the gas flow physics knowledge by proposing division of the impinging gas jet structure into three distinct flow regions: the free jet region, the stagnation flow region and the wall jet region [4]. The model he proposed illustrates the airflow rate profile of an impinging gas jet which is directly related to the heat transfer coefficient in the region of contact between the impinging jet and the surface of a heated dense solid body. The three main flow regions are shown in Fig. 1 [4].



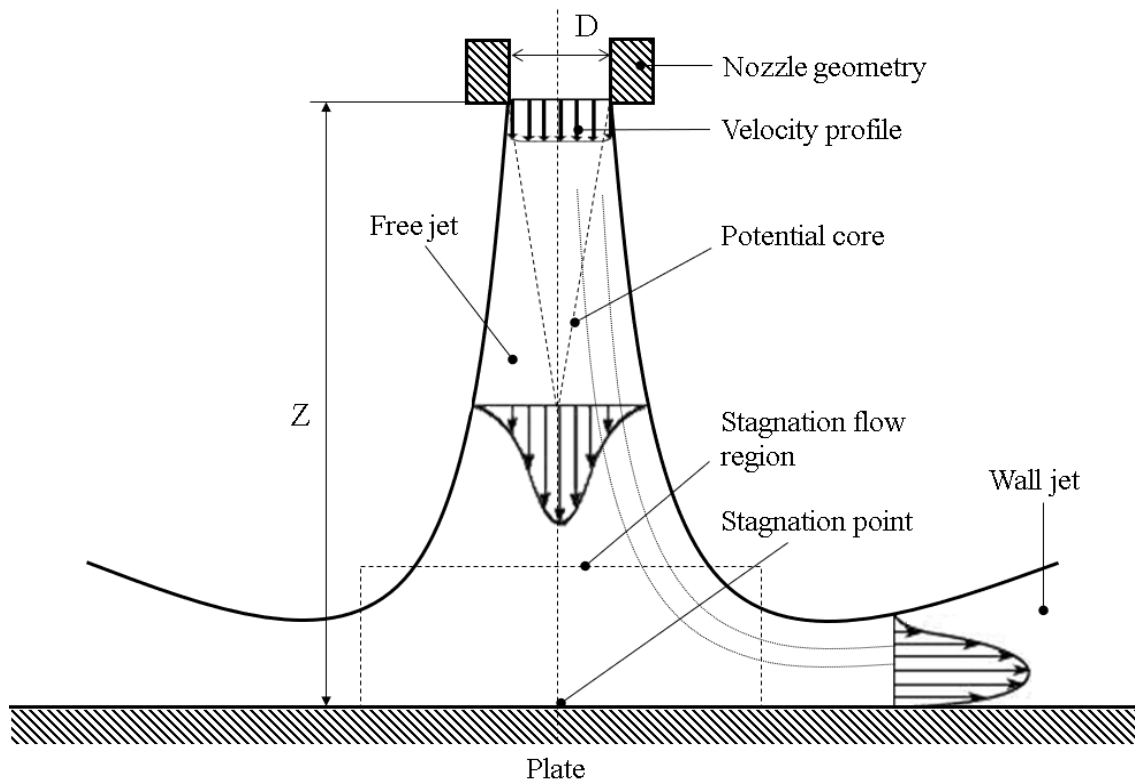


**Figure 1.** Schematic representation of a vertical impinging gas jet [4].

### 1.1. The Free Jet Region.

In this region spreading with increasing gas jet rate is observed against the fluid from the surrounding space. In the region of the potential core which is found at a distance up to 4 – 6 times the nozzle diameter no changes are observed in the speed and temperature of the impinging gas jet.

### 1.2. The Stagnation Flow Region

This region is characterized by the presence of a stagnation point. The pressure has a local maximum value at the stagnation point.

### 1.3. The Wall Jet Region

For the wall jet region formation of a laminar boundary layer is characteristic which turns into a turbulent jet at a distance 1-2 times the diameter of the nozzle [4].

Accuracy evaluation of the numerical analysis against the results of the experimental measurements of the heat transfer process can be carried out using the dimensionless  $Nu$ . The  $Nu$  is a universal way of expressing the efficiency of a heat transfer process and have been used in a number of scientific works as a dimensionless criterion for comparing heat transfer processes [9].

Due to the increasing complexity of the tasks solved with the help of virtual twins, in-depth analyzes are necessary to evaluate the accuracy of different software programs used for modeling the impinging gas jets. Despite the accumulated extensive practical experience in using impinging gas jets in our daily life, significant difference often occur between the basic research results in this direction and the digital twins used. In this regard a number of software program validations have been carried out in recent years. K Thiel in [6] compared three *CFD* programs, *Fluent*, *CFX* from *ANSYS* and *Hybrid*. In this case, experimentally obtained values NACA0012 were studied. The used meshing tools were: *ICEM CFD*, *GAMBIT* and *CENTAUR*. The results show that the processed validation cases from each program can be partly solved in different ways. S Spring [6,12] examined the correlation between

the simulation values of heat transfer obtained by *CFX-5.7.1* and the selected turbulence models using a single impinging gas jet for validation on a flat plate and selection of two  $Z/D$  distances of 6 and 12 at different  $Re$ .  $Z$  defines the distance between the nozzle exit and a heat conducting solid plate, and  $D$  defines the inner diameter of the nozzle. F Ahmet et al. [12] examined the influence of the nozzle geometric parameters on the way of the impinging jet spreading using *CFD* simulations. A more complex experimental case was considered by P S Penumadu and A G Rao [8] which involves the interaction of 225 impinging gas jets passing through nozzles with a diameter of 400  $\mu\text{m}$ . They limited the overall dimensions of the region under investigation by using a digital twin characterized by symmetrical boundary conditions. The results of this study provide an insight into the physical processes of impinging gas jet spreading and their mutual influence.

## 2. Selection of test cases

The results accuracy evaluation of an impinging gas jet numerical study of solid surfaces was performed by direct comparison of the dimensionless  $Nu$  values obtained by experimental and simulation way. The  $Nu$  was selected in this case as a criterion for assessing accuracy of the simulation results because it adequately represents the correlation between geometric and energy parameters of the heat transfer process. In the experiment under consideration, the parameters describing the heat transfer process efficiency depend entirely on the nozzle geometry, formed impinging jet, temperature of the solid body around which the gas flows, the type of medium used for the experiment, and its initial characteristics. The case corresponds to the experimental set-up at  $Re = 23000$ ,  $Z/D = 2$ . Characteristic of this experiment is that besides the initial maximum  $Nu$  in the stagnation flow region a secondary maximum is observed at a distance  $2D$  corresponding to twice the nozzle diameter for all experiments performed at  $Z/D = 2$  [1-2] [7]. The studies of S Spring [11] and F Ahmet [12] and the corresponding local  $Nu$  obtained experimentally [1-2] were used for verifying the authenticity of *CFD* code of *STAR-CCM+*.

## 3. Computational details

To perform a numerical analysis of the accuracy of *STAR-CCM+ 6.04.014*, a digital twin of the experimental model was used shown in point 2 [1-2].

### 3.1. Domain and boundary conditions

During the simulation the boundary and initial conditions of the digital twin did not undergo change. Reading of the local  $Nu$  was performed by reaching a quasi-stable equilibrium state of iterations. Two turbulence models were validated - *SST* and  $v^2f$ . The models were selected after preliminary analysis of the survey results obtained with other software products such as *Fluent*, *CFX* [6] and *Fluent* [7-8] [13-14] which show satisfactory accuracy against other popular turbulence models such as  $k-\epsilon$  and  $k-\omega$  for the respective experimental set-up.

The digital twin from Fig. 2 is characterized by the following Domain and boundary conditions: a circular cross section of the air nozzle  $D = 26$  mm, impinging jet velocity  $u_j = V_0$  at  $Re = 23000$  and kinematic viscosity at jet temperature  $T_j = 293,15$  K.

The working medium in this system was air at an initial state corresponding to a temperature  $T_u = 293,15$  K and a static pressure  $p_u = 101325$  Pa. Non-permeable thermally conductive solid body was used which is located parallel to the nozzle exit cross section at a distance  $Z = 2D$ . The initial temperature of the body was  $T_j = T_u$  which was subjected to a constant external thermal influence of a specific wall heat flux  $q_w = 300$   $\text{W}/\text{m}^2$ . Additionally, modification of the numerical domain was done with the purpose of using hardware resources efficiently and accelerating the time of obtaining the results of the digital twin investigation while maintaining the accuracy of the results. This was possible because of the axial symmetry of the system relative to the axis of the nozzle.

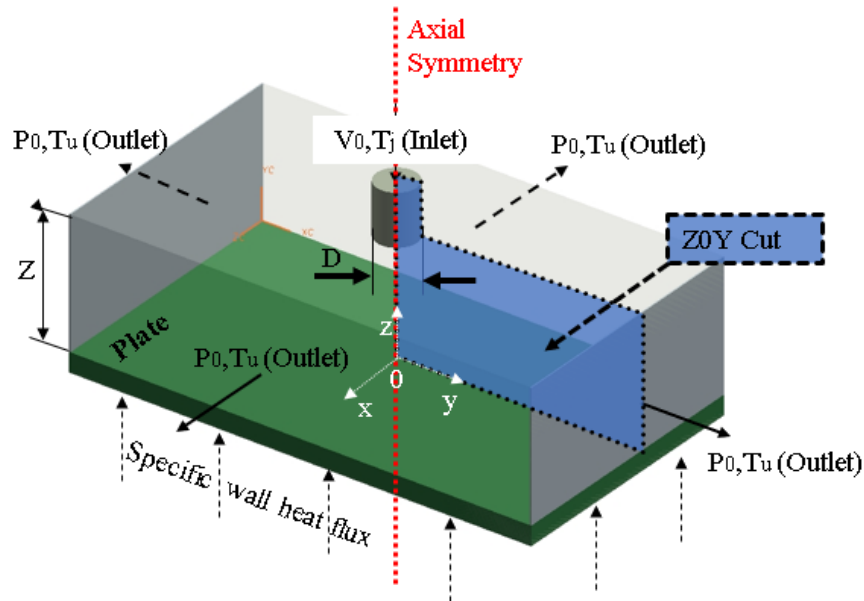


**Figure 2.** Numerical modeling and boundary conditions of the digital twin.

The two-dimensional domain *XOZ Section* shown in Fig. 2 is extrapolated from the basic digital twin and has the shape shown in Fig. 3. Further modification of the domain from Fig. 3 is fulfilled for better stability of the iterations in the numerical examination process. The result is a three-dimensional domain with a thickness  $D_s$  corresponding to the thickness of one cell of the numeral domain (Fig. 4).

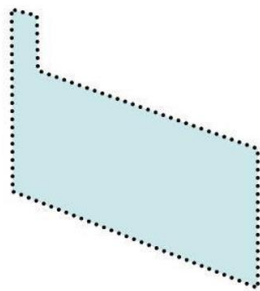


**Figure 3.** Two-dimensional view of the domain ZOY Section.

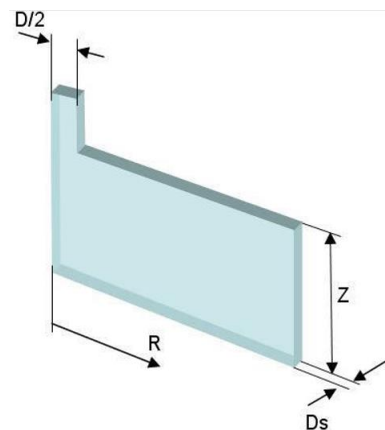


**Figure 4.** Three-dimensional view of the numerical domain.

The boundary areas of the digital twin in the computing domain are defined according to their physical characteristics, respectively Wall, Axial Symmetry, Wall (Heat Flux), Inlet, Stagnation Inlet and Pressure Outlet (Fig. 5).

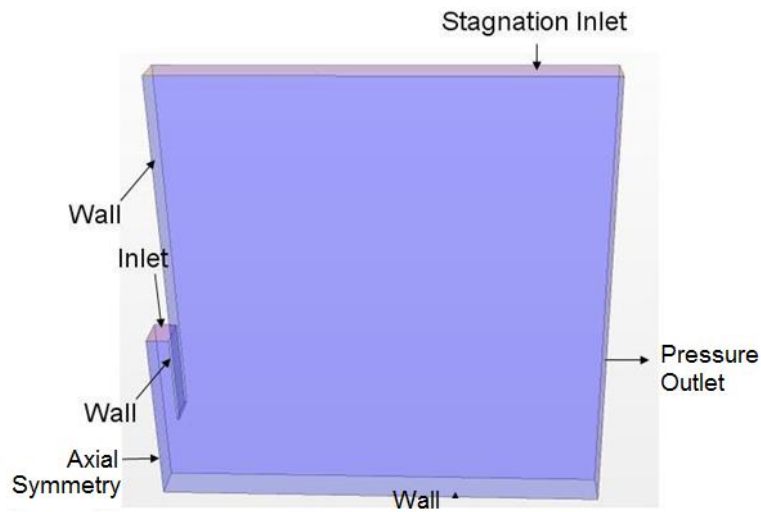
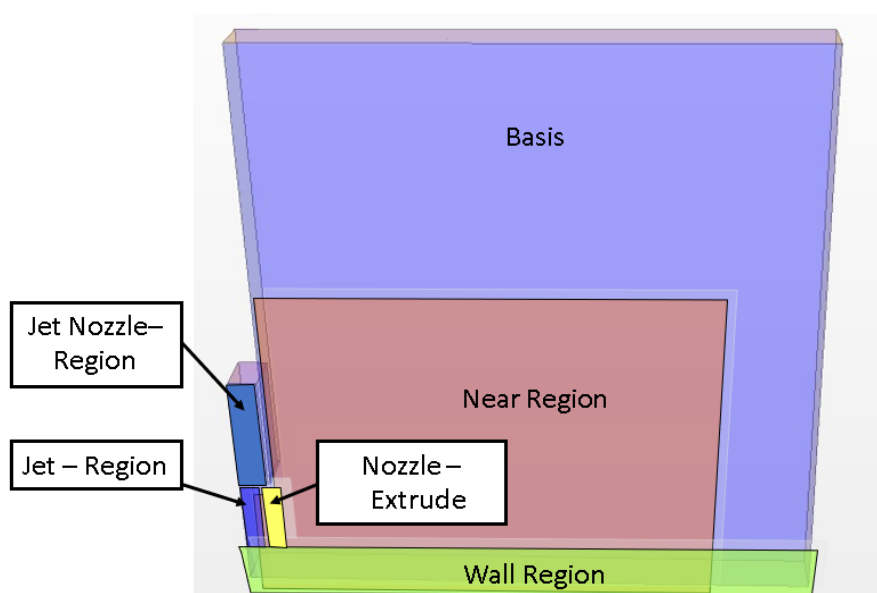


**Figure 5.** Boundary areas of the digital twin.

### 3.2. Grid generator

The grid is generated in the commercial solver *STAR-CCM+* version 6.04.014. Trimmed cells with base length of 2 mm are used. A prismatic layer of 6.6 mm thickness in 200 layers with a coefficient of expansion of 1,03 and a Dimensionless wall distance  $y^+ = 0,065$  is defined near the wall.

Fig. 6 shows the computing domain divided into several zones. Additionally, smaller areas such as "Jet Nozzle Region", "Jet Region", "Nozzle Extrude" and "Wall Region" are integrated to the regions with large areas such as "Basis" or "Near Region". These areas are linked to each other through a refined grid which improves the results quality.



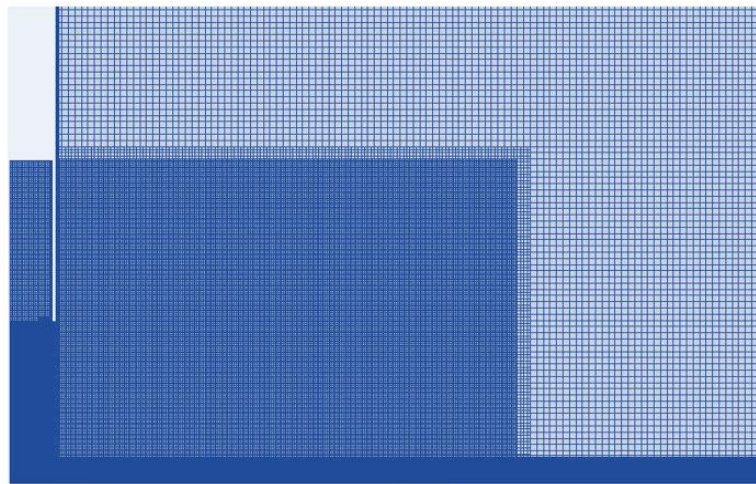
**Figure 6.** The location of the additional meshed areas.

Table 1 presents the ratio of the cell size in all areas relative to the basic thickness of the cell expressed as a percentage.

**Table 1.** The ratio of the cell size in the different areas relative to the basic thickness of the cell of 2 mm.

Area	Ratio (%)
Basis	100
Near Region	25
Jet Nozzle-Region	30
Jet-Region	20
Nozzle-Extrude	10
Wall Region	10

After analysis of the grid for independence of the result from its size, a choice was made which was used for subsequent analyzes of a modified digital twin with the number of cells 153912 (Fig. 7).



**Figure 7.** Three-dimensional view on a grid for the study of heat transfer between impinging gas jets and solid surfaces.

#### 4. Numerical prediction and evaluation of turbulence models

Two pre-selected turbulence models ( $\nu^2f$  and  $SST$ ) were used to perform the simulation results analysis which are integrated into the  $STAR-CCM +$  software. In both cases the studies of the turbulence models were performed in completely identical domain and boundary conditions of the digital twin. The obtained results were validated with the experimentally determined values described in [1-2] whose numerical values are shown in Fig. 8.

At the stagnation point a very good match is observed between the measured and the numerical values for  $Nu$  of the model  $\nu^2f$ . In this area, the maximum deviations - more than 20 % between the  $SST$  model and the experimental values are observed.

The numerical prediction of the flow and heat transfer of the two turbulence models shows a deviation up to 18 % after the first maximum at a distance  $R/D = 1,3$  and reaching a secondary maximum at  $R/D = 2,5$ . The model  $\nu^2f$  provides values that are closer to the maximum obtained in the experiment against  $SST$ . The  $\nu^2f$  model provides a well-expressed secondary maximum against  $SST$ . The average distribution of the  $Nu$  is characterized by a difference of less than 9%.

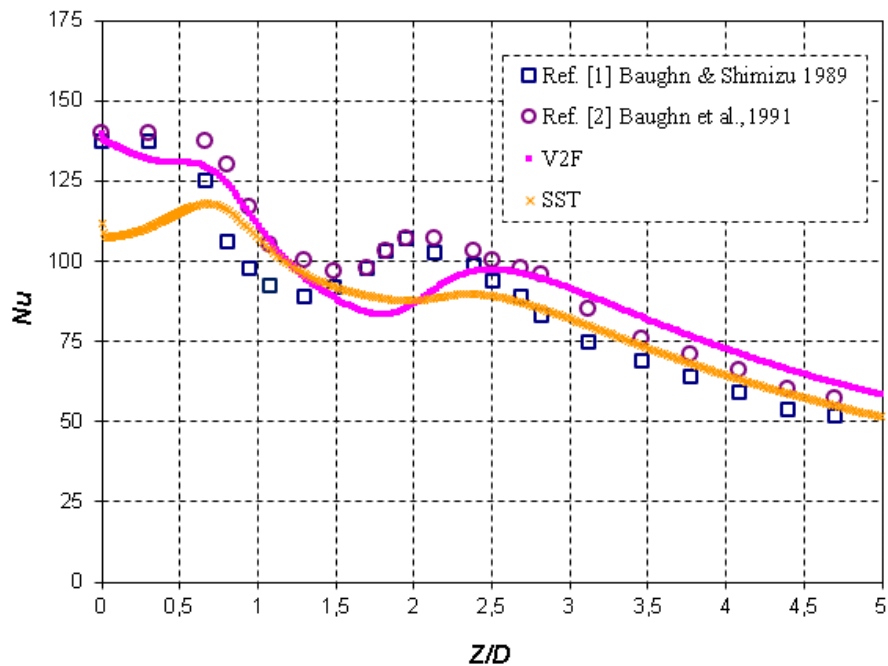


**Figure 8.** Local  $Nu$  distributions predicted by  $v2f$  и  $SST$  turbulence models by  $Re = 23000$  and  $Z/D = 2$  in comparison to experimental data from [1-2].

For the spreading profile of the velocity magnitude (Fig. 9) a non-homogeneous transition is observed in the contact region between the air jet and the ambient air for both turbulence models. This may be due to the transition between two meshed areas with different cell sizes, despite the used cell independence analyzes.

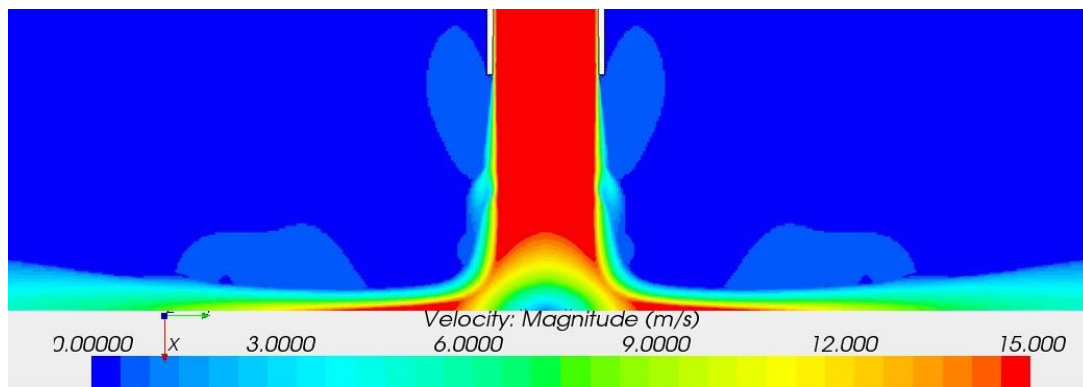


**Figure 9.** Visualization of the magnitude velocity distribution ( $SST$  turbulence model).

## 5. Conclusion

The two turbulence models show satisfactory comparison and reproduction of the  $Nu$  values on the considered metal plate surface despite the deviations from the secondary maximum location. Forming a primary and secondary maximum can be observed in both models, and in  $v2f$  the obtained numerical values for the first maximum coincide completely with the performed experiments. The maximum difference between the local results obtained for the  $SST$ -model is below 21 % if these extremes are located for that model in the area of the first maximum, and for  $v2f$  in the area of the second maximum those differences do not exceed 10 %. The  $v2f$  model achieves good consistency at the stagnation point

where the difference is less than 0,5 %. At  $R/D = 2,5$  to 4, the SST-model also achieves results with a difference of less than 1% compared to the measured values.

Reproduction of the primary and secondary maximum is achieved in both turbulence models in the considered application area. The  $v^2f$  model shows a mean deviation of the numerical results against  $Nu$ 's average number across the whole range which is less than 7,9 %. For the SST-model this value is 8,8 %. Both models can provide satisfactory heat transfer performance in case of impinging gas jet at  $Re = 23000$ .

### Acknowledgments

This work was supported by the European Regional Development Fund within the OP “Science and Education for Smart Growth 2014-2020”, Project Competence Centre “Smart Mechatronic, Eco-And Energy Saving Systems And Technologies“, № BG05M2OP001-1.002-0023.

The authors would like to thank the Research and Development Sector at the Technical University of Sofia for the financial support.

### References

- [1] Baughin J W and Shimizu S 1989 Heat transfer measurements from a surface with uniform heat flux and an impinging jet *J. Heat Transfer*, **111** 1096–1098
- [2] Baughn J W, Hechanova A E and Yan X 1991 An experimental study of entrainment effects on the heat transfer from a flat surface to a heated circular impinging jet *J. Heat Transfer* **113** 1023–1025
- [3] Florschuetz W, Truman C R, Metzger D E 1981 Streamwise flow and heat transfer distributions for jet array impingement with crossflow *J. Heat Transfer* **103(2)** 337-342
- [4] Martin H 1977 Heat and mass transfer between impinging gas jets and solid surfaces *Advances in Heat Transfer Academic Press New York* **13** 1–60
- [5] Perry K 1954 Heat transfer by convection from a hot gas jet to a plane surface *Proc. Inst. Mech. Eng.* **168** 775-784
- [6] Thiel K 2006 Vergleich des Lösungsverhalten der CFD - Programme: FluentTM, CFXTM und Hybrid *Graduate Thesis on the Institute of Aerospace Thermodynamics University of Stuttgart* 24-47
- [7] Zu Y Q, Yan Y Y, Maltson J D 2007 CFD prediction for confined impingement jet heat transfer using different turbulent models *Proc. of ASME Turbo Expo 2009 Power for Land, Sea and Air Orlando Florida USA* GT2009-59488
- [8] Penumadu P S, Rao A G 2017 Numerical investigations of heat transfer and pressure drop characteristics in multiple jet impingement system *J. Appl. Thermal Engineering* **110** 1511–1524
- [9] Spring S 2010 Numerical Prediction of Jet Impingement Heat Transfer *PhD thesis Institute of Aerospace Thermodynamics on the University of Stuttgart* ISBN 978-3-86853-811-3 35-54
- [10] Beltaos S 1976 Oblique impingement of circular turbulent jets. *J. Hydraulic Research* **14** 17–36
- [11] Spring S, Weigand B, Krebs W, Hase M 2006 CFD Heat Predictions of a Single Circular Jet impinging with Grossflow. *AIAA ASME Joint Thermophysics and Heat Transfer Conference San Francisco California USA* **9** 3589
- [12] Ahmet F B, Tucholke R, Weigand B, Meier K 2010 Numerical investigation of heat transfer and pressure drop characteristics for different hole geometries of a turbine casing impingement cooling system *14th International Heat Transfer Conference Washington DC USA IHTC* **14-22817** 99-212
- [13] Penchev S, Seyzinski D, Stanchev J 2006 Modeling the flow in test section of wind tunnel UT-1 *Journal of the Technical University at Plovdiv “Fundamental Sciences and Applications” Plovdiv Bulgaria* **13(8)** 82-86
- [14] Panayotov H, Hafizoğlu S 2014 Airfoil aerodynamics investigation using automated CFD analysis *6<sup>th</sup> Sc. Conf. BulTrans 2014 Sozopol Bulgaria Proc.* 86-90